Ground penetrating radar survey and tracer observations at the West Pearl Queen carbon sequestration pilot site, New Mexico

Thomas H. Wilson, Arthur W. Wells, J. Rodney Diehl, Grant S. Bromhal, Duane H. Smith, and William Carpenter*, National Energy Technology Laboratory (NETL), Pittsburgh, PA & Morgantown, WV & *West Virginia University Department of Geology and Geography*

The potential for leakage of injected CO_2 at carbon sequestration sites is a significant concern in the design and deployment of long-term carbon sequestration efforts. Effective and reliable monitoring of near-surface environments in the vicinity of these sites is essential to ensure the viability of sequestration activities as well as long term public and environmental safety. Identification of geological features such as faults, fracture zones, and solution enhanced joints that might facilitate release of injected CO_2 back into the atmosphere is a key step in this process. This study reports on near-surface geological and geophysical characterization efforts conducted at the Department of Energy National Energy Technology Lab (NETL) West Pearl Queen carbon sequestration pilot site in southeastern New Mexico (Figure 1) and their use in uncovering possible mechanisms associated with escape of small amounts (10^{-13} liters) of perfluorocarbon tracers injected with the CO_2.

In this pilot test, 2100 tonnes of CO_2 were injected into the Shattuck sandstone member of the Permian Queen Formation early in 2003. Tracers injected with the CO_2 were detected within a few days of injection and continued to escape for several months following injection. Geological and geophysical characterization of the near-surface environment in the vicinity of the injection well incorporated lineament interpretations (Figures 2 and 3) and a detailed ground penetrating radar survey of a circular area extending out 300 meters from the injection well (see Figure 4). The near-surface geology consists of a few-feet thick veneer of late Pleistocene and Holocene sand dunes

covering the middle Pleistocene Mescalero caliche (a soil horizon hardened by precipitation of carbonate from soil solution). The lineament study incorporated interpretation of black and white aerial photos from 1949, digital orthophotos, and Landsat TM imagery. Lineament analysis reveals distinct northeast and northwest trending lineament sets. The GPR survey reveals a nearly continuous blanket of caliche beneath the area that varies in thickness from approximately 0 to 5 feet. Numerous fault-like features, amplitude anomalies, and reflection gaps disrupt the caliche. Some of these disruptions are traceable over distances of 25 to 200 meters and their aerial distribution shows some association with the distribution of tracers detected in the near-surface at the site. Caliche topography suggests that runoff across the caliche surface was channeled. The observations also suggest the caliche layer has undergone significant karstification. Solution features, if present, could serve as near-surface escape routes.

Lineament Analysis. Lineament interpretations were conducted at three different times during a 2 year period in the vicinity of the West Pearl Queen pilot site. Lineaments mapped at a detailed local scale are shown on an orthophoto of the area (Figure 2). Rose diagrams of lineament trends (Figure 3) reveal that the majority of lineaments fall into clusters with orientations of N40-50W and N40-60E. The origins of these lineaments are unknown. Field observations reveal that lineaments generally coincide with more sparsely vegetated strips within the dune complex. Lineaments may be associated with enhanced surface drainage over solution features within the caliche. Larger depressions within the dune complex at the site also trend NW-SE or NE-SW. These depressions may be simple wind-scoured blow-outs but could also be dolines formed by solution and

subsidence of the underlying Mescalero caliche (*Phillips, 1987, The prospects for regional groundwater contamination due to karst landforms in Mescalero caliche at the WIPP site near Carlsbad, New Mexico: Dissertation, University of Oregon, 316p*).

Ground Penetrating Radar Survey. A detailed ground penetrating radar survey was conducted of the area surrounding the Stivason #4 injection well (Figure 4) to image the Mescalero caliche. The survey was conducted using a Sensors and Software, Inc. Smart Cart with 250MHz antenna. Approximately 10 kilometers of survey lines were collected across the site with approximately 25 cm trace spacing. In general, survey lines were 100 meters long, spaced at 25-meter intervals, and laid out in a radial pattern centered at the injection well (see Figure 4). High relief dunes northeast and east of the injection well prevented acquisition of GPR data in those areas. Karst features in this area of the Mescalero Plain are largely the result of caliche dissolution (Phillips, 1987). The objectives of the GPR survey were twofold: 1) to determine if the caliche layer could be detected and effectively mapped using GPR methods and, 2) if so, to estimate the thickness of the caliche, identify possible fracture zones, faults, and solution features that might serve as high permeability pathways that could facilitate lateral transmission and vertical escape of CO_2 back into the atmosphere.

Prominent reflection events observed in GPR profiles (Figures 5) are interpreted to arise from the near surface caliche layer. Stubbs (*2004, Oral Communication*) reports widespread distribution of the Mescalero Caliche throughout the area. The presence of the layer is confirmed by a near-surface gamma ray log in the Stivason #5 well just 400

meters east of the injection well (Figure 6), and also in numerous hammered holes used to place the capillary adsorption tube samplers (CATS).

Radar wave velocity in the dune cover was estimated from near-surface diffraction events (Figure 7) to be roughly 0.19 m/ns. Depths to the caliche calculated from reflection travel times indicate that the top of the caliche horizon lies about 4 to 10 feet beneath the surface across the area. Surface elevation variations at the site are largely responsible for the short wavelength travel time variations common to the GPR profiles in the survey (e.g., Figures 5 and 7). Although detailed elevation data were not collected along individual GPR profile lines, elevation data were available across the site on a 110 foot grid collected for a 3D seismic survey of the area (*Benson, written communication, 2003*). Topography or structure on the caliche structure (Figure 4) was calculated using two-way travel times to the caliche reflection event and surface elevation data. Reflection travel times were converted to depths, and both the depth and elevation data were interpolated onto a regular 10 meter grid. The depth grid was then subtracted from the elevation grid to obtain the structure or topography on the old caliche surface (Figure 4). Numerous topographic features appear on the old caliche surface. In general the caliche layer drops approximately 20 feet from 3700 feet in the north to 3680 feet in the south over a distance of roughly 600 meters. Topographic lows to the south and southwest would have channeled runoff during heavy rains in wetter climatic intervals following formation of the caliche.

Caliche thickness (Figure 8) was computed using a velocity of 0.15 m/ns (0.5ft/ns). Diffractions clearly arising from the base of the caliche were not observed. Use of a 0.15m/ns interval velocity yields variations in the thickness of the caliche of 0 to 4

feet. Conversion using an interval velocity of 0.11 m/ns, which would be more typical of carbonate rocks, yields thickness variations of from 0 to a little more than 3 feet. Interpretation of the gamma ray log from the Stivason #5 well (Figure 6), suggests the caliche may be from 5 to 7 feet thick at that location. While this 0.15m/ns velocity may be high for this carbonate zone, it does provide thickness estimates consistent with the only data point we have from the site. Thinned areas to the south and southwest coincide with lows on the caliche surface and suggests that carbonate dissolution was focused in this area.

A variety of additional features were observed in the radar profiles across the area. These included abrupt offsets, changes of thickness, missing reflections, and anomalous reflection amplitude. While a large number of possible offsets were interpreted across the area, very few appeared to be associated with features that might correlate from one profile to the next. Interpreted faults with apparent line-to-line correlations are shown in the caliche structure and thickness maps (Figures 4 and 8). Missing caliche reflections (e.g. Figure 9) are observed only in a few areas at the site. However, the caliche thickness map (Figure 8) reveals extensive areas where its thickness is a foot or less. Areas where the caliche has been completely eroded or dissolved are outlined in red (Figure 8) and tend to be concentrated in the topographic low and thinned areas south and southwest of the injection well.

γ Ray and density porosity logs. 3D models of the γ ray log response from nine wells in the area surrounding the injection well reveal a region of low γ ray response approximately 40 – 50 feet thick near the injection well (Figure 10). The diameter of this

zone is about 600 meters. The γ ray response of the unconsolidated Pleistocene deposits overlying the Triassic bedrock is generally quite low and suggests that near surface sediments are dominated by clean sands. Density porosity computed from the bulk density logs using a quartz matrix density of 2.65 gm/cm^3 is on average between 0.61 and 0.65 in the upper 300 feet at the site. Shallow density logs are available only for the Stivason #4 and #5 wells. Together, the porosity and γ ray observations suggest the injection well is surrounded by clean and relatively high porosity sands particularly in the upper 40 to 50 feet of the near-surface surrounding the injection well.

Tracer Studies. Leakage detection experiments conducted at the pilot site were designed and undertaken by Art Wells and Rod Diehl (Pittsburgh NETL). They positioned capillary adsorption tube samplers (CATS) in a radial pattern centered about the Stivason Federal #4 injection well (e.g. Figure 4). A total of 40 CATS were placed at the site and their locations are shown by black dots on the orthophoto views of the area (e.g. Figure 8). Individual CATS were placed in metal tubes at depths of approximately two meters. The CATS were specially designed to detect minute amounts (10^{-13} liters) of perfluorocarbon tracers injected with the CO_2. The base of the tube was left open to allow for diffusion of soil gas into the sampler. CATS were left in the ground for different periods to measure changes in tracer concentration as a function of time through the CO_2 injection process. Three different perfluorocarbon tracers were injected into the CO_2 stream. These included perfluorodimethylcyclohexane (PDCH), perfluorotrimethylcyclohexane (PTCH), and perfluorodimethylcyclobutane (PDCB).

CATS exposed for a 54 day period revealed the presence of anomalies in the distribution of tracers detected around the injection well (Figures 11-13). Elevated concentrations of PDCH and PTCH (Figures 11 and 12) were detected by CATS located northwest of the injection well. Elevated concentrations of PDCB (Figure 13) were detected by CATS located southwest of the injection well. The PDCH tracer was added 24 hours after CO_2 injection was initiated. PTCH was added nine days after injection started, and the PDCB tracer was not injected into the CO_2 stream until 21 days after CO_2 injection commenced. Measured concentrations of PDCH (the first tracer injected into the CO_2 stream) at 6, 10, and 54 days following injection revealed that tracer release was incremental through the period of time during which CO_2 injection took place. PDCB concentrations reported in this study are for the 54 day exposure time. CATS placed at the site during the soaking period following CO_2 injection reveal a decline in concentration for all tracers. This decline was most significant for the PDCBs. PDCB, with the highest diffusion constant, tends to be present in larger amounts, and drops to background levels more rapidly than the other tracers.

GPR interpretations suggest the presence of a fault/fracture zone extending northwest of the injection well that coincides with the trend of elevated tracer concentrations. Dissolution of the caliche may be enhanced along this trend and lead to a greater concentration of solution pipes and fractures and thus increased connectivity between solution voids in this direction. If this is the case, higher permeabilities may facilitate rapid transport of CO_2 to the surface along this northwest zone. The possible association of features in the caliche layer to elevated concentrations of PDCB observed southwest of the well may be facilitated by the processes that led to thinning of the

caliche observed in this area. The caliche surface is structurally low to the south and southwest and the thinning could be a direct consequence of increased dissolution of the caliche associated with channeled runoff through this area. Observations during the post injection period reveal a significant decline in PDCB concentration to the southwest. During the same time period there was a much smaller relative drop in PDCH and PTCH concentrations to the northwest.

Potential Transport Mechanisms. The results of the GPR survey suggest possible mechanisms that could have facilitated near surface tracer leakage. An additional potential mode of transport to the near-surface sampling locations is through the atmosphere. If the tracer leaks at the surface, or if it reaches the target stratum and leaks back through the entire subsurface, it mixes with the atmosphere. Wind currents and Fickian diffusion processes both contribute to the tracer movement once it is in the atmosphere, and it is possible that the tracer will diffuse (or flow by atmospheric pumping) back into the ground to the monitoring stations. Ideally, one would place the CATS deep enough that atmospheric concentrations would be negligible; however, with sandy soil only a few feet thick, that may not be possible. With data on average wind speed and direction, an atmospheric transport model that incorporates both advection and dispersion in the vertical and horizontal directions can be used to simulate this process. At the West Pearl Queen site the wind blew steadily out of the southwest during tracer injection. This would most likely contaminate CATS to the northeast. However, contamination in this area was not observed. The pattern of tracer release observed at the site cannot be explained by atmospheric transport.

A more likely means of transport of injected CO_2 to the surface is from leakage around the well bore, either through the injection well or nearby abandoned wells. If the cement in the well bore degrades or does not bond well with the surrounding rock, then conduits can form around the well and CO_2 can rise rapidly through the subsurface. This type of transport can be modeled to some degree with a traditional reservoir simulator. We will be performing simulations in the near future for the West Pearl Queen field to see how leakage around the injection well could contribute to vertical CO_2 migration.

Leakage of hydrocarbons above natural hydrocarbon reservoirs is often observed (*e.g. Tedesco, 1995, Surface Geochemistry in Petroleum Exploration: Chapman and Hall, 206p*). Microseepage is assumed to result from vertical migration of hydrocarbons to the surface through fracture networks and high permeability zones. A similar process may work for carbon dioxide seepage, wherein the CO_2 leaks upward under the influence of buoyant forces through relatively high permeability fracture zones into more permeable formations above. CO_2 was injected into the Shattuck sand at a pressure of approximately 2900 psi. While this is considerably below lithostatic pressure (~ 5300 psi) it is well above hydrostatic pressure (~ 2060 psi). If relatively permeable fracture zones penetrate the Shattuck and extend to the surface, injection pressure combined with buoyancy could drive CO_2 back to the surface. Experience in enhanced oil recovery (EOR) projects has shown that such transport may be fairly rapid (as soon as 18 months); however, the overall flowrate is very low, because the volume of the fractures through which the gas travels is very small. We are currently developing a discrete fracture code to model vertical migration of CO_2 through fracture networks.

The vadose zone is the region of the subsurface that lies near the ground surface and is above the water table (i.e., not saturated with water). At the West Pearl Queen site, the vadose zone is about 60m deep. The primary mechanism of transport in the vadose zone is diffusion (Klusman, 2002), unless significant pressure changes occur at or near the ground surface, e.g., a leak in a pipe or a rapid change in atmospheric pressure. Diffusion of CO_2 and tracer can occur both radially—outward from the well—and upward from leaks below the water table. In the following example, radial variations in tracer concentration are modeled using the diffusion equation:

$$\frac{\partial c}{\partial t} = D\left(\frac{\partial^2 c}{\partial x^2} + \frac{\partial^2 c}{\partial y^2}\right)$$

Here D stands for the coefficient of diffusion at location x, y; c stands for concentration; and t is time. Several simulations were run to determine the maximum extent of tracer diffusion over the 54 day time period in the experiments. In these simulations, the permeability is represented by the coefficient of diffusion, which was allowed to vary between 0.1 and 0.01cm^2/s. The simulation shown in Figure 14 was obtained using a heterogeneous permeability field in which diffusion coefficients in the above range were distributed randomly throughout the model. Results of the simulation (Figure 14) indicate that the process of diffusion through the vadose zone cannot account for the rapid migration of tracers to sample locations beyond 100 meters or so.

GPR interpretations suggest that oriented fracture systems and solution features may influence flow through the caliche layer. Oriented lineament sets identified in imagery suggest the presence of enhanced permeability trends in the veneer of sands

overlying the caliche. Future simulations will model flow from the well bore into a layer with diffusion coefficients that define enhanced permeability along fracture zones. These simulations will incorporate information from the GPR survey which suggests the presence of NW-SE and NE-SW fracture or high permeability trends and allow us to evaluate whether mode rapid migration of tracers to out to distances of 300 meters or so could occur.

The possible influence of producing wells in the surrounding area has also been evaluated as a potential source of contamination. Wells that were producing during CO_2 injection are located more than 1000 feet from the injection well. Reservoir simulations reported by Pawar et al. (*2004, Numerical modeling of CO_2 Sequestration in a depleted oil reservoir, Proceedings of the 4rd Annual Conference on Carbon Sequestration, NETL, Alexandria, VA*) suggest that CO_2 migration 80 days after injection stopped did not extend more than 200 feet from the injection well into the surrounding Shattuck sandstone. In addition, although production in nearby wells continued, tracer concentration dropped after CO_2 injection was completed.

Conclusions. Surface and near-surface characteristics of the West Pearl Queen pilot carbon sequestration site were investigated using remote sensing and ground penetrating radar methods to identify possible migration pathways associated with escape of perfluorocarbon tracers injected into the CO_2 stream. Elevated concentrations of tracers were observed along trends northwest and southwest of the injection well. Analysis of remote sensing imagery revealed prominent lineament trends (NW-SE and NE-SW) in the thin veneer of sands that blanket late Pleistocene soils. The radar survey revealed

significant discontinuity and structure within the near-surface late Pleistocene Mescalero caliche. Karstification of this carbonate horizon during the 400,000 years since its formation probably produced high permeability pathways through the caliche in the form of solution pipes, and solution enlarged joints and fracture zones. A prominent fault-like feature observed in the radar images of the caliche may facilitate migration of injected CO_2 into near-surface areas northwest of the injection well. Topography on the old caliche surface suggests that channeled runoff during wetter climatic periods may have enhanced dissolution and thinning of the caliche to the southwest. Lineament trends and patterns of heterogeneity observed in the Mescalero caliche coincide roughly with the NW and SW tracer leakage trends. Simulations of tracer diffusion through the near surface suggest that the process of diffusion through a heterogeneous surface layer cannot explain the extent of tracer release observed at the site. In this particular case contamination appears to be associated with injection process and not to contamination from nearby producing wells. This view is supported since CATS retrieved after injection ceased revealed reduced tracer concentrations while production continued in surrounding wells. The characteristics of near surface heterogeneity inferred from the remote sensing study and GPR survey will serve as inputs in the design of reservoir models that will incorporate discrete fracture networks to simulate pressure-driven vertical and horizontal microseepage at the West Pearl Queen pilot site, wherein the tracers may flow much farther than in the diffusion-driven case.

This study provides an evaluation of several issues that can arise in the context of monitoring and verification of CO_2 sequestration. Leakage detection is essential to the

success of these endeavors since leakage rates of less than 1% per year could, in the long term, return much of the injected CO_2 back into the earth's atmosphere.

Acknowledgements

The authors would like to thank Charles Byrer of NETL for his time and support of our efforts in this project. Our thanks to Norm Warpinski for providing geophysical logs from the pilot site, and to Bob Benson for providing elevation control over the site. Appreciation is also extended to John Hawley, John Kennedy, Bruce Stubbs, and Ron Broadhead for helpful discussions and perspectives on the geology the pilot site and surrounding region.

Suggested Reading. See the March 2003 issue of Geotimes (S. Friedmann, Storing Carbon in Earth; Geotimes Staff, Demonstrating Carbon Sequestration at http://www.geotimes.org/mar03/) for a discussion of basic issues and ongoing carbon sequestration pilot projects. White, D. J., et al. (2004) Greenhouse gas sequestration in abandoned oil reservoirs: The International Energy Agency Weyburn pilot project, *GSA Today*. White, C., et al. (2003) Separation and capture of CO_2 from large stationary sources and sequestration in geological formations – coalbeds and deep saline aquifers, in *J. Air &Waste Management Assoc.* provides a comprehensive overview of several issues associated with long term carbon sequestration activities. For an overview of DOE's Geologic Sequestration Research programs and projects visit *http://www.fe.doe.gov/programs/sequestration/ geologic/.*

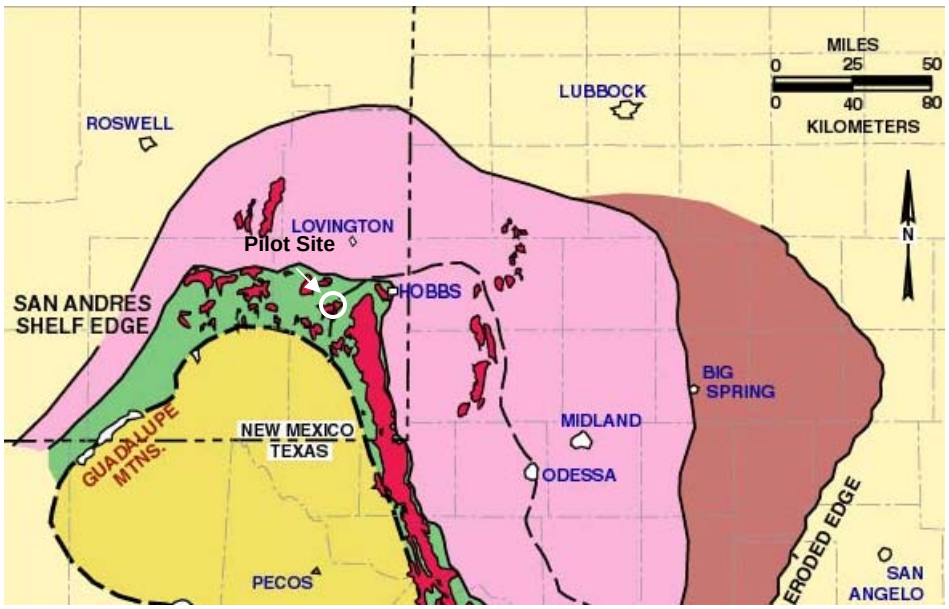

Figure 1: The pilot site is located approximately 25 miles southwest of Hobbs, NM. Oil and gas fields in the area are highlighted in red. Map taken from Ward (1986) (*http://geoinfo.nmt.edu/staff/scholle/guadalupe.html An introduction and virtual geologic field trip to the Permian reef complex, Guadalupe and Delaware mountains, New Mexico-West Texas*).

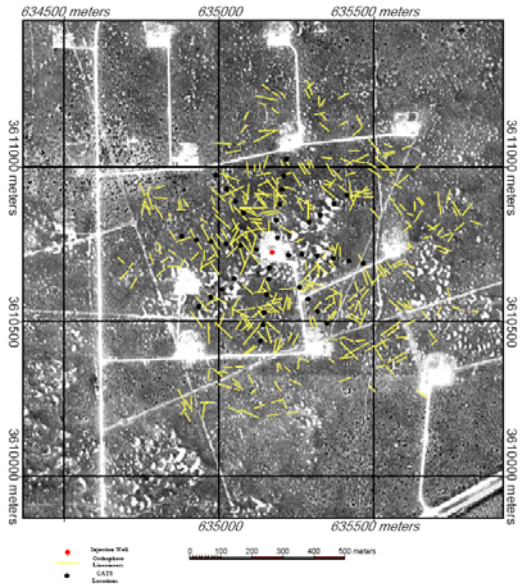

Figure 2: Short photo lineaments (yellow) are shown on an orthophoto of the test site. The locations of injection well (red) and capillary absorption tube samplers (black) are spotted on the photo.

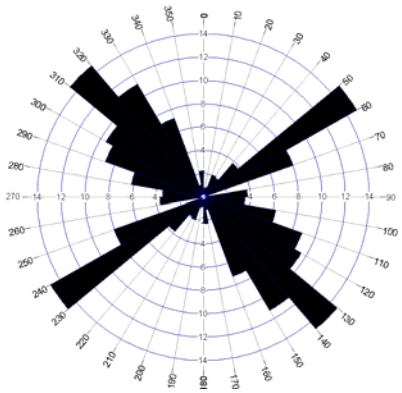

a.

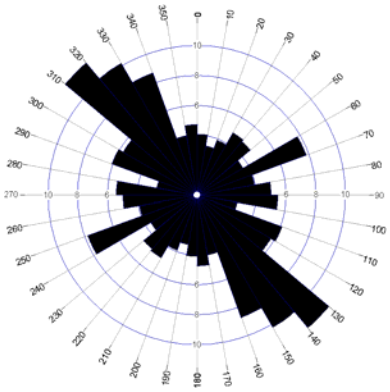

b.

Figure 3: a) Rose diagram of photolineaments picked from a contrast enhanced digital copy of a 1949 black and white aerial photo of the area surrounding the West Pearl Queen pilot injection well. Lineaments identified in this exercise consisted of sharp, distinct, usually dark colored linear features picked at a detailed scale (1.3km x 1.3km area). N = 225. b) Rose diagram of lineament trends observed in the vicinity of the pilot injection well on the digital orthophoto of the area reveals a dominant N45W lineament trend in the area. These lineaments consist of relatively high-contrast narrow linear features observed on the orthophoto. N = 536

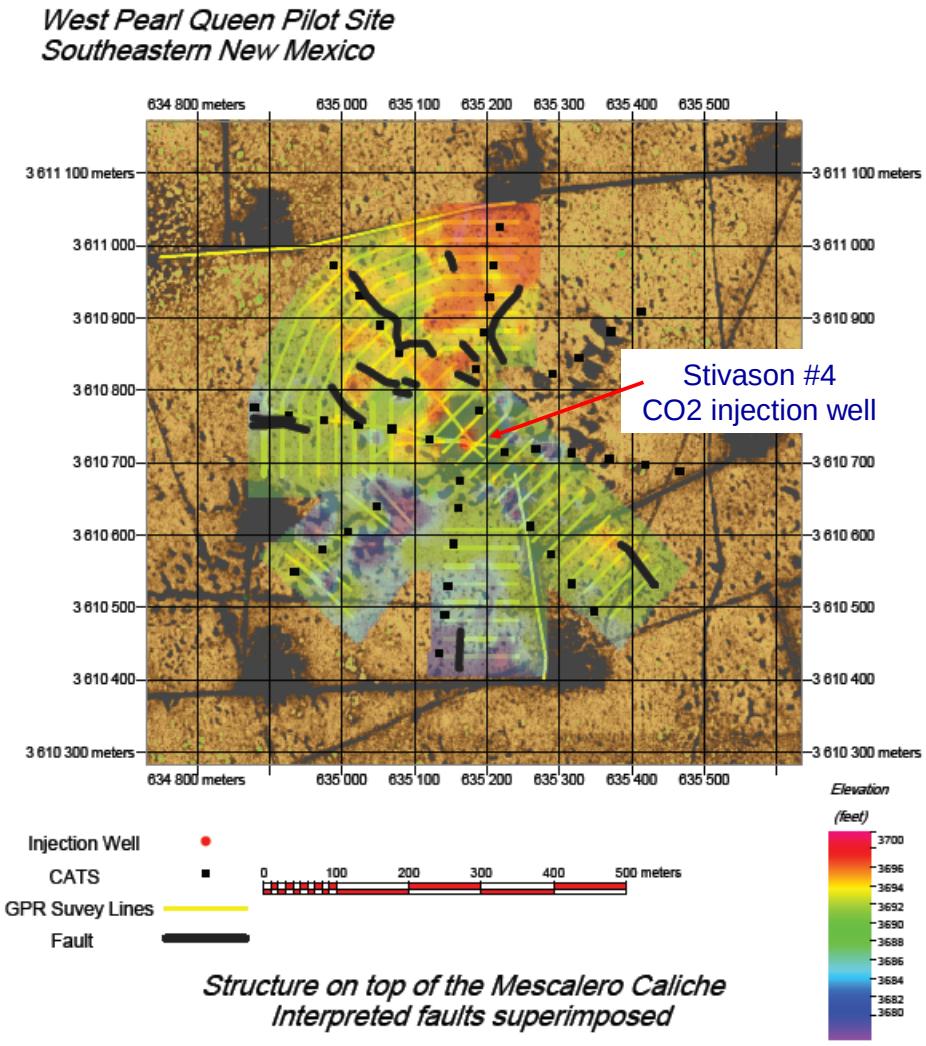

Figure 4: Structure of the Mescalero caliche is superimposed on an orthophoto of the injection site. GPR survey lines are shown in yellow. Locations of the injection well, CATS, and interpreted faults are also shown.

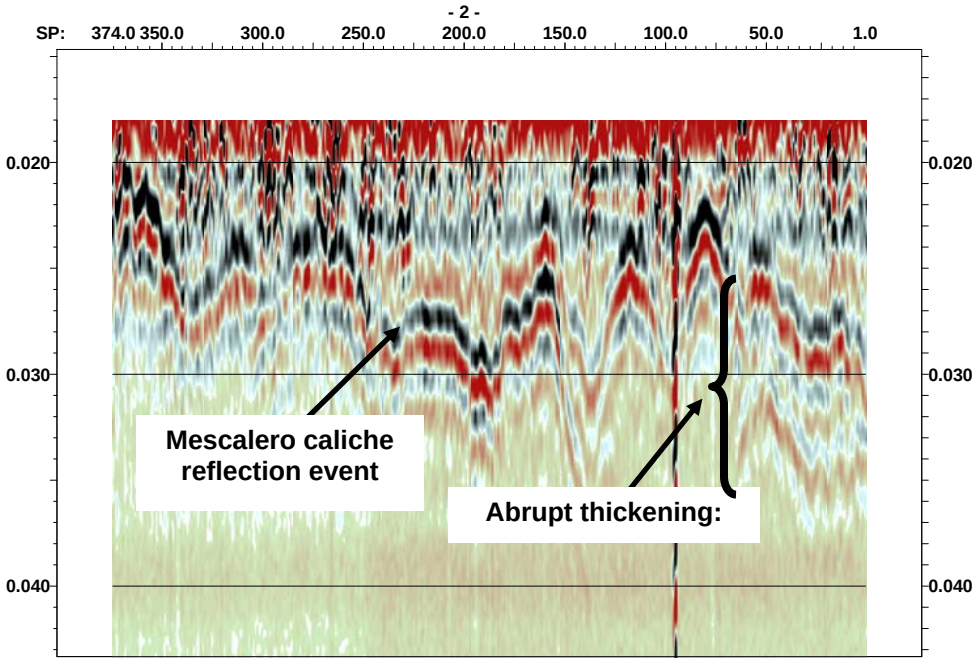

Figure 5: GPR profile located 275 meters northwest of the injection well illustrates the general character of the reflection events from the Mescalero caliche observed across the site.

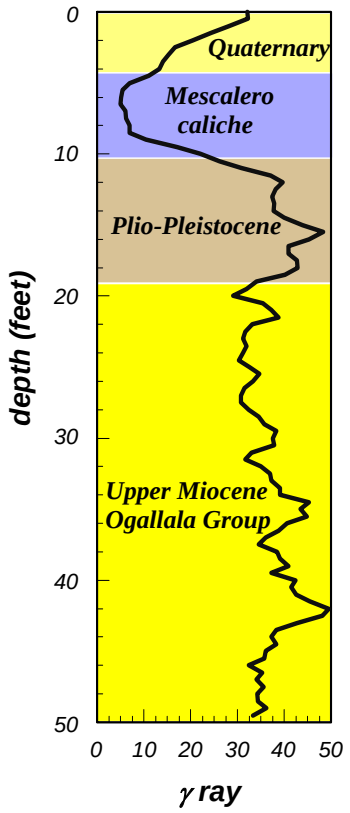

Figure 6: Gamma ray log from the Stivason #5 well 400 meters east of the Stivason #4 injection well. The low gamma ray response between 4 and 9 feet subsurface is associated with the Mescalero caliche.

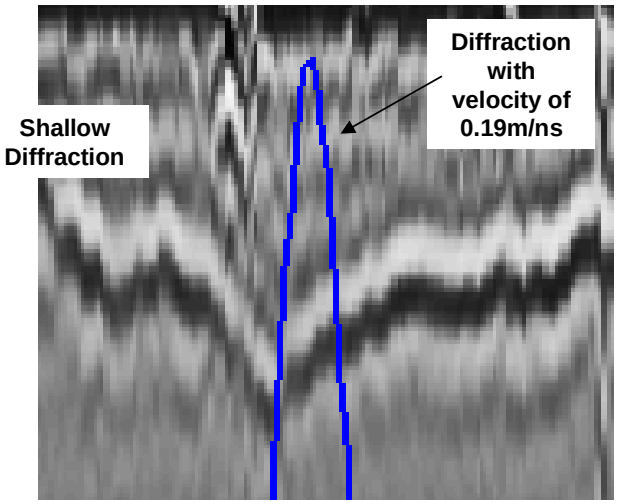

Figure 7: Diffraction hyperbola having a velocity of 0.19 m/ns is displayed next to a shallow diffraction originating in the near surface sand cover.

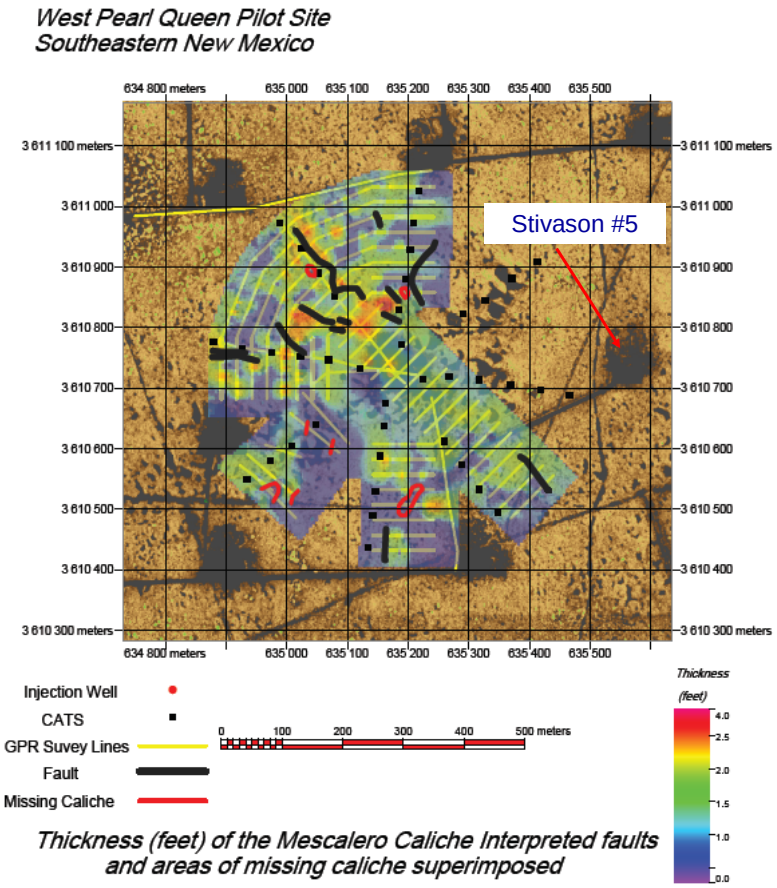

Figure 8: Thickness of the Mescalero caliche estimated from interpreted two-way radar reflection travel times through the caliche using an interval velocity of 0.15m/ns. Interpreted faults/fracture zones and areas of missing caliche are highlighted.

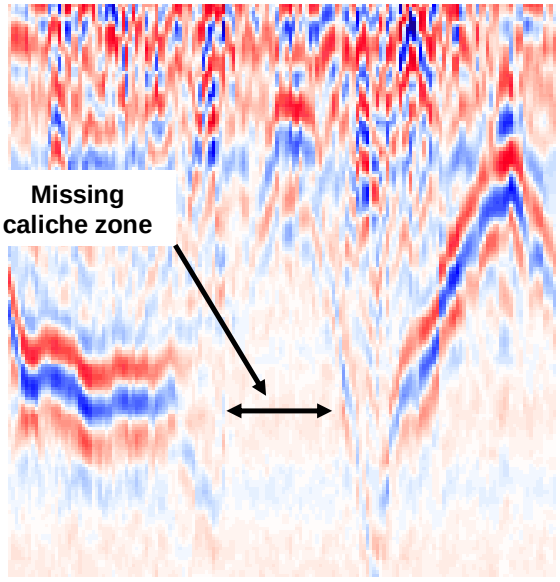

Figure 9: Abrupt thinning and disappearance of caliche reflection events are illustrated in this GPR profile.

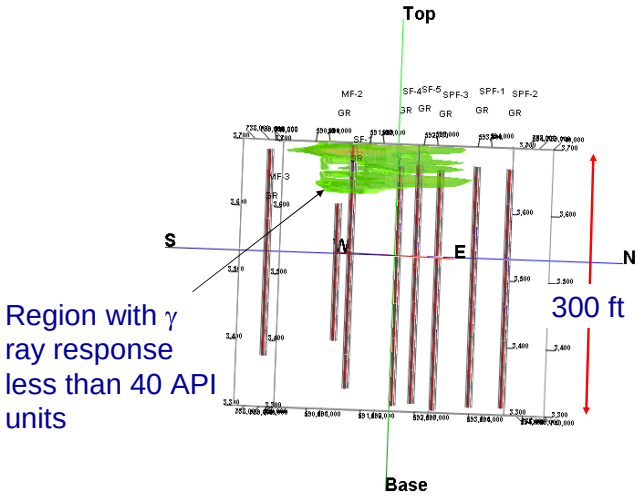

Figure 10: 3D model of the near surface γ ray response reveals the injection well is surrounded by a thick zone of clean sand. The model selectively displays intervals having a γ ray response less than or equal to 40 API units.

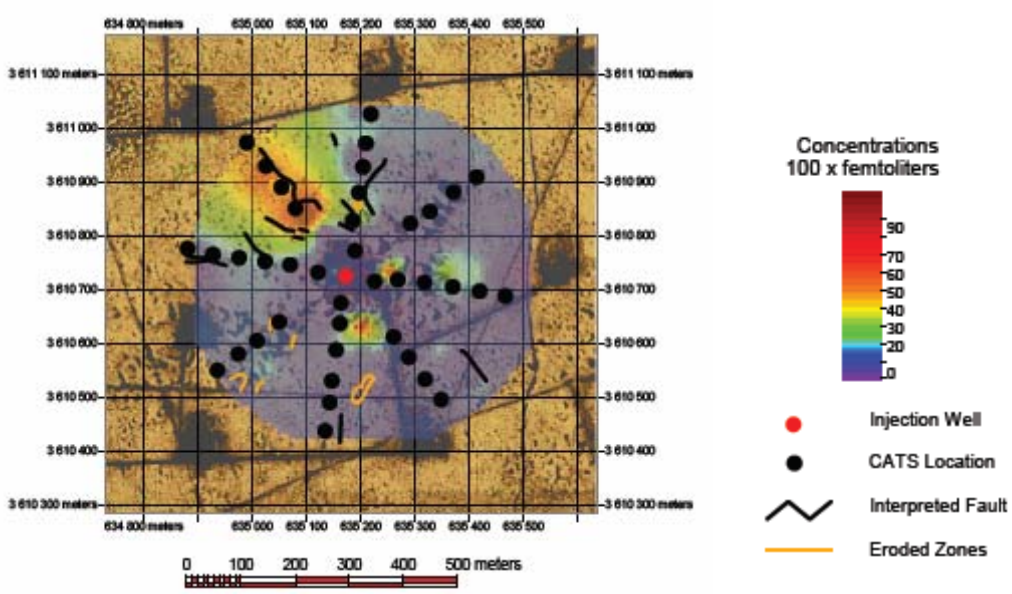

Figure 11: Concentrations of PDCH measured during a 54-day exposure period are superimposed on an orthophoto of the pilot site. The locations of the injection well, CATS, interpreted faults, and eroded caliche areas are shown for reference.

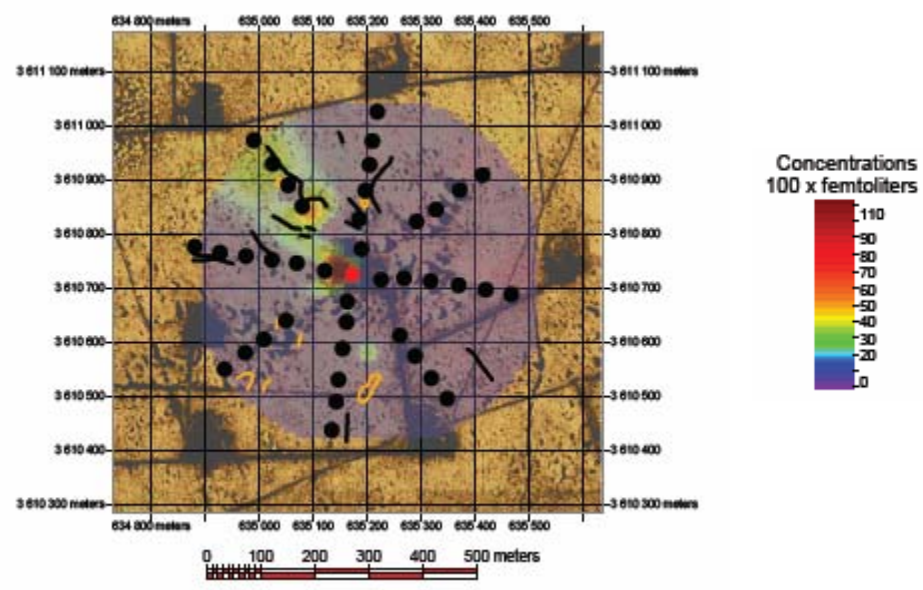

Figure 12: PTCH concentrations measured during the 54-day exposure period.

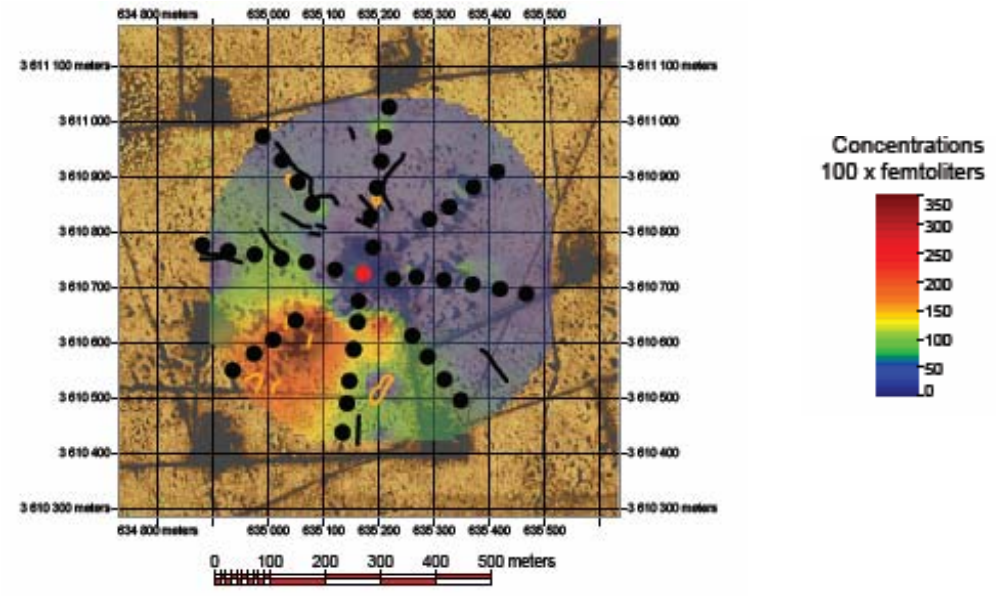

Figure 13: PDCH concentrations measured during the 54 day exposure period.

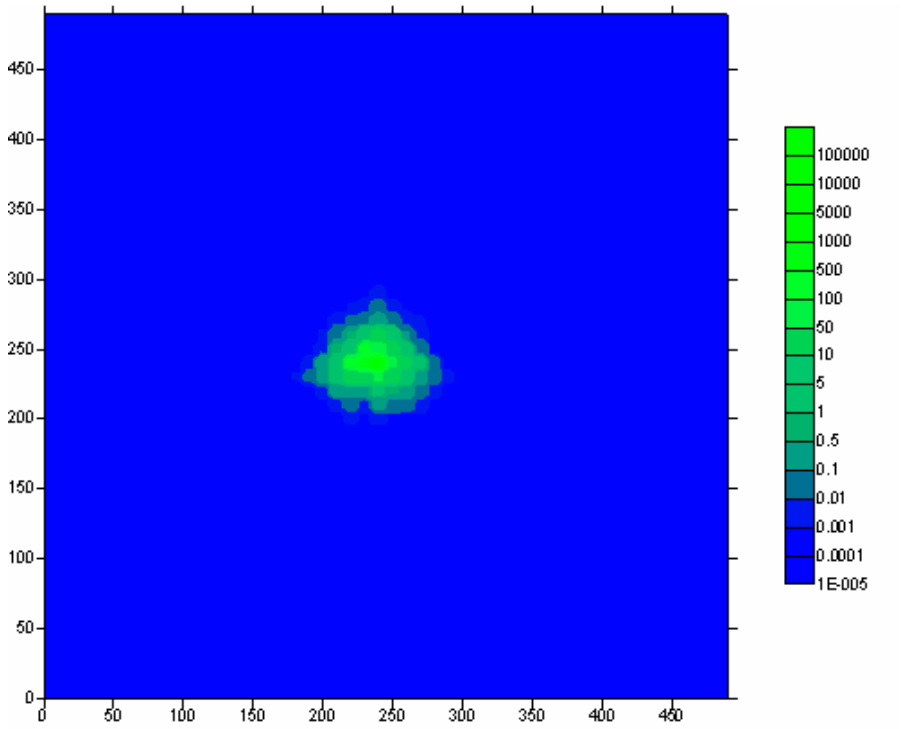

Figure 14: Diffusion pattern of tracer concentrations after 54 days associated with initial release of 3000ppt from a well located at the point (250,250). Concentration units are in pptv; map distances are in meters.